JOURNAL OF CATALYSIS, 99, 415–427 (1986)

Control of the Catalytic Activity of Tungsten Carbides

I. Preparation of Highly Dispersed Tungsten Carbides

JACQUES LEMAÎTRE,[1] BENOÎT VIDICK, AND BERNARD DELMON

Groupe de Physico-Chimie Minérale et de Catalyse, Universtié Catholique de Louvain, Place Croix du Sud 1, B-1348 Louvain-la-Neuve, Belgium

Received February 21, 1984; revised July 8, 1985

A study of the preparation of carbides using hydrous oxide precursors is presented. Two different precursors ($WO_3 \cdot H_2O$ and hexagonal $WO_3 \cdot xH_2O$), obtained by homogeneous precipitation from ammonium tungstate solutions, have been converted into carbides after preliminary dehydration and reduction steps. The carburization step was performed either in pure CO or in CO–CO_2 mixture (CO/CO_2 ratio = 10 : 1). Carburization in pure CO always resulted in the deposition of free carbon on the surface of the carbides, as was shown by XPS analysis. The use of a CO/CO_2 mixture made it possible to minimize the coverage of the carbide particles by free carbon, probably as a result of a slackening of the CO dismutation reaction. Hence, the amount of free carbon in excess over the quantity necessary to convert W_2C to WC was maintained at the lowest possible level. The so obtained carbides proved to be extremely well dispersed (30 m^2/g). They appeared to consist of particles which were pseudomorphic with the starting oxides. A passivation treatment, consisting of contacting the samples with diluted oxygen at 21°C, was found necessary in order to prevent their spontaneous ignition in air.

INTRODUCTION

In the past 15 years, transition metal carbides have attracted increasing interest from investigators working in the field of catalysis. Analogies between their catalytic properties and those of noble metals have been observed. Thus, Muller and Gault (*1*) showed that metallic tungsten had an increased activity for the isomerization of hydrocarbons, after an induction period; furthermore, the selectivity of the reaction was characteristic of metals such as Pd and Pt. Similarly, Sinfelt and Yates (*2*) observed that metallic Mo became increasingly active with time for the hydrogenolysis of ethane. In both cases the formation of a superficial carbide was suggested by the results. Later on, Levy and Boudart (*3*) observed qualitative similarities between the behaviour of Pt and WC with respect to their chemisorption properties, as evidenced by hydrogen-oxygen titration experiments. Since then, the potential field of application of tungsten carbides as heterogeneous catalysts has grown considerably (*4–9*).

In another direction, owing to its good chemical inertness in acidic solutions (*10*), WC has found application as a catalytic electrode for the anodic oxidation of hydrogen in fuel cells (*11–13*). Furthermore, it has been shown that the electrochemical activity of WC was not affected by small amounts of CO and H_2S (*14–16*). This suggests that WC might have an unusual resistance to poisoning by compounds, especially sulfided ones, which are known to depress dramatically the activity of noble metal catalysts.

The literature shows that the catalytic properties of WC samples may vary considerably according to their origin and preparation method. Many factors are thought to influence the catalytic activity of tungsten carbides, among which two are most frequently cited, namely the presence of oxygen, possibly in solid solution, and either an

[1] To whom correspondence should be addressed.

0021-9517/86 $3.00

excess or a lack of carbon in the surface layer of the solid. Thus, according to Ilchenko (*5*), the catalytic activity of the transition metal carbides for hydrogen oxidation is higher for samples showing a lower heat of oxygen chemisorption. Similarly Böhm (*17*) showed that the activity of WC for the electrooxidation of hydrogen was favorably influenced by its oxygen content. He therefore proposed a mild oxidation treatment (at 300°C in oxygen) of WC electrodes in order to increase their activity. The presence of a carbon layer on the surface of WC catalysts would inhibit their activity (*18, 19*) while a superficial carbon deficiency would increase it (*20*).

Unfortunately, contradictions found in the literature show that the above interpretations do not account for all the experimental data. Thus, Ross and Stonehart (*18*) found that the activation treatment suggested by Böhm (*17*) could have an effect which was either favorable or detrimental on the activity of WC anodes, according to their preparation method. Kojima and coworkers (*7*) showed that WC became active in hydrogenation only after a thermal activation treatment at high temperature, during which oxygen was found to desorb from the surface of the catalyst. Contradictions also exist with respect to the effect of carbon. Thus, carburization at low temperature has been recommended by Armstrong *et al.* (*11*) in order to increase the amount of surface defects in the solid and hence its catalytic activity, whereas Ross and Stonehart (*18*) have shown that WC samples obtained by carburization at low temperature were inactive due to surface contamination by free carbon.

The discrepancies among the activities reported either for WC electrocatalysts or for contact catalysts can be explained, at least partially, by their diverse origins and ways of preparation. This latter parameter has been studied by Ross and Stonehart (*18*) and by Nikolov *et al.* (*21, 24*). These authors have shown that the activity of WC catalysts can vary by a factor of 20, depending on the nature of the precursor and the carburization conditions used for their preparation (temperature and atmosphere).

A systematic study of the different preparation factors of WC, including the nature of the precursor and the final carburization conditions, is therefore very relevant.

The present work reports part of the results obtained in a program aimed at the control of the preparation of WC catalysts, in the hope to vary at will some characteristic parameters (e.g., carbon content, surface oxygen, crystallinity, specific surface area) and hence to obtain clearer evidence about their actual influence on the catalytic activity of these compounds.

The results of the investigations will be presented in three parts. Part I is concerned with the preparation of highly dispersed tungsten carbides. Part II will present the control and characterization of the surface state of WC samples, particularly the effects of treatments with H_2 and O_2. Finally, Part III will describe catalytic properties of WC samples and tentatively correlate them with the surface properties and preparation factors of the samples.

This paper (Part I) presents a study of the influence of the carburization conditions (gas-phase composition, temperature, time) and the nature of the hydrous oxide precursor used, on some of the characteristics of the final carbides (phase composition, contamination by free carbon, specific surface area). The results will be interpreted in the light of thermodynamic data in the WO_3-WO_2-W-W_2C-WC-C system. Finally, a tentative reaction scheme for the transformation of W_2C to WC will be proposed.

EXPERIMENTAL

Materials

Highest purity tungstic acid (H_2WO_4) from U.C.B. and 25% aqueous ammonia pro analysi from Merck were used as received. H_2 (N30), CO (N37), CO_2 (N45), and Ar (N46) were used as supplied by Air Liquide; the purity of the gases is codified by Air Liquide as follows: H_2 (N30)—$H_2 + D_2 > 99.90\%$ ($O_2 < 10$ ppm and $H_2O < 10$ ppm); CO (N37)—CO > 99.97% ($O_2 < 10$

ppm and $H_2O < 5$ ppm); CO_2 (N45)—$CO_2 > 99.995\%$ ($O_2 < 10$ ppm and $H_2O < 5$ ppm); Ar (N46)—Ar > 99.996% ($O_2 < 3$ ppm and $H_2O < 5$ ppm). The gas used for the passivation treatment was a "Type 2 Accurate Mixture" of O_2 ($5 \pm 0.05\%$) and He (95%), also from Air Liquide.

Preparation of the Samples

The hydrous oxide precursors were prepared (*25*) using a homogeneous precipitation technique described previously by Kervyn *et al.* (*26*). Full details about the development of the preparation and treatments of the precursors prior to the carburization reaction are given in Ref. (*25*). Only those features relevant to the samples studied in the present series of papers will be presented below.

The impossibility to wash Na out of tungsten hydrous oxides prepared by precipitation from Na tungstate solutions, and the very limited solubility of well-crystallized ammonium paratungstate salts made it necessary to prepare soluble ammonium tungstate using the following procedure. A stoichiometric amount of H_2WO_4 was added to an aqueous solution of NH_3. The mixture was boiled and refluxed for 10 min under continuous stirring. After cooling to ambient temperature, the solution was freeze-dried (Virtis Freezemobile 12 apparatus). An amorphous ammonium tungstate, very soluble in water, was thus obtained.

Two different kinds of tungsten hydrous oxides, referred to below as "yellow" ($WO_3 \cdot H_2O$, labeled as Ye) and "white" ($WO_3 \cdot \frac{1}{3}H_2O$, labeled as Wh) phases have been prepared by ageing acidified tungstate solutions.

Yellow phase. Twenty milliliters of 1 *M* HNO_3 (p.a.) were added in a polyethylene bottle to 30 ml of a 0.01 *M* ammonium tungstate (A.T.) solution (final pH = 0.35); the bottle was stoppered, kept for 30 min at room temperature and placed in an oven for 4 h at 60°C.

White phase. Twenty milliliters of 0.1 *M* HNO_3 (p.a.) were added to 30 ml of a 0.05 A.T. solution (final pH = 1.4) in a polyethylene bottle; the bottle was stoppered and the sample was immediately placed in an oven for 4 h at 90°C.

After cooling to ambient temperature, the precipitates were separated from their mother solution by centrifugation at 5000 rpm for 10 min. The supernatant layer was removed and the solid was resuspended in distilled water (75 ml/g). Each precipitate was washed 3 times in this way. Finally, the solid was dispersed in distilled water and the suspension was freeze-dried.

Prior to carburization, the samples had to undergo a reduction treatment in well defined conditions, in order to preserve as much as possible their original texture. All the thermal treatments described below were performed in a quartz-made, fixed bed, flow-through reactor (i.d. = 18 mm).

Reduction. Approximately 0.4 g of the hydrous oxide precursor was placed in the reactor and held by a quartz wool plug. The reactor was purged with argon prior to establishing a flow of H_2 (15 l/h). The temperature was then raised from ambient up to 500°C at a rate of 1°C/min and the reduction was continued for 5 h at this temperature. When it was desired to examine the intermediate metallic tungsten, a flow of Ar was established at the end of the reduction step and the reactor was cooled to ambient temperature; the sample was then submitted to the passivation treatment described below.

Carburization. At the end of the reduction step Ar was flowed through the reactor instead of H_2. The temperature was then raised at 1 °C/min from 500°C up to the carburization temperature. At this point, the carburization mixture was sent to the reactor. After the desired carburization time had elapsed, the reactor was purged with Ar and cooled to ambient temperature.

Passivation treatment. After cooling to ambient temperature, the argon flow was substituted by a 5% O_2 in He mixture (10 liters/h) for 2 h. This treatment was found to be necessary to prevent spontaneous ignition of the samples in air. It was checked that this passivation treatment did not alter the specific surface area of the samples (*25*).

Analytical Methods

X-Ray diffractometry. X-Ray diffractograms were obtained using a Philips Norelco PW1051 apparatus (Cu$K\alpha$ radiation, d = 1.5148 Å, Ni-filtered). The molar fraction x of WC in a W_2C–WC mixture was calculated from X-ray data as follows:

$$x = h_1/(h_1 + h_2),$$

where h_1 and h_2 are, respectively, the peak heights of the most intense reflections of WC (d = 1.88 Å) and W_2C (d = 2.28 Å).

Surface area. Specific surface areas were calculated from N_2 adsorption measurements at 77 K, using the BET method. The measurements were made in a vacuum microbalance, the samples being first outgassed to constant weight at 120°C. The specific surface area determination of a nonpassivated metallic tungsten sample has been done on a sample which had been reduced *in situ* in the microbalance.

Electron microscopy. Transmission electron micrographs were obtained on a AEI EM6G microscope using an acceleration voltage of 100 kV. Scanning electron micrographs were recorded on a JEOL Temscan 100 CX, using an accelerating voltage of 60 kV. The samples were dispersed in high-purity methanol using an ultrasonic vibrator and deposited on carbon films supported on standard AEI copper grids.

X-Ray photoelectron spectroscopy (XPS). Measurements were carried out with a Vaccum Generator ESCA 3 spectrometer equipped with an Al anode ($h\nu$ = 1486.6 eV) operated at 20 mA and 14 kV. The signal-to-noise ratio was improved by using a Tracor Northern signal averager. The residual pressure inside the spectrometer was 1.3×10^{-7} Pa.

Nomenclature. The samples will be designated as follows: A-WC-x, where A (Wh or Ye, see above) indicates the nature of the precursor and x stands for the conversion to WC (mol%) of the sample. Samples carburized in pure CO will be denoted A-WC-x-CO.

RESULTS

Characterization of the Precursors and Metallic Intermediates

The freeze-dried yellow and white tungsten hydrous oxides were identified by X-ray diffraction as $WO_3 \cdot H_2O$ and hexagonal $WO_3 \cdot \frac{1}{3}H_2O$, respectively. Their respective specific surface areas are presented in Table 1. The micrographs of Fig. 1 show that the white precursor consists of fine acicular particles packed into aggregates about 0.25 μm in diameter (micrograph c), while the yellow precursor is in the form of rounded platelets about 0.25 μm thick and 0.5 to 1.5 μm in diameter (micrograph d).

The specific surface areas of the samples at intermediate stages of their preparation are presented in Table 1. Micrographs a and b of Fig. 1 show that both samples are pseudomorphic with respect to their respective hydrous oxide precursor.

Study of the Carburization Reactions

Carburization in pure CO. The effects of temperature, time, and nature of the precursor on the phase composition of the samples obtained upon carburization in pure CO are presented in Table 2. Experiments 1 to 3 show that the conversion to WC of the white precursor goes through a maximum with time at 750°C. Under the

TABLE 1

Specific Surface Areas of the Precursors and their Metallic Intermediates

Nature of the precursor	Specific surface area (m^2/g)		
	Precursor	Calcined (500°C)	Metallic W
White	82 ± 2	36 ± 2	71 ± 2[a]
			70 ± 2[b]
Yellow	16 ± 1	13 ± 2	64 ± 2

[a] Passivated sample.

[b] Sample reduced *in situ* in the microbalance, prior to the specific surface area measurement.

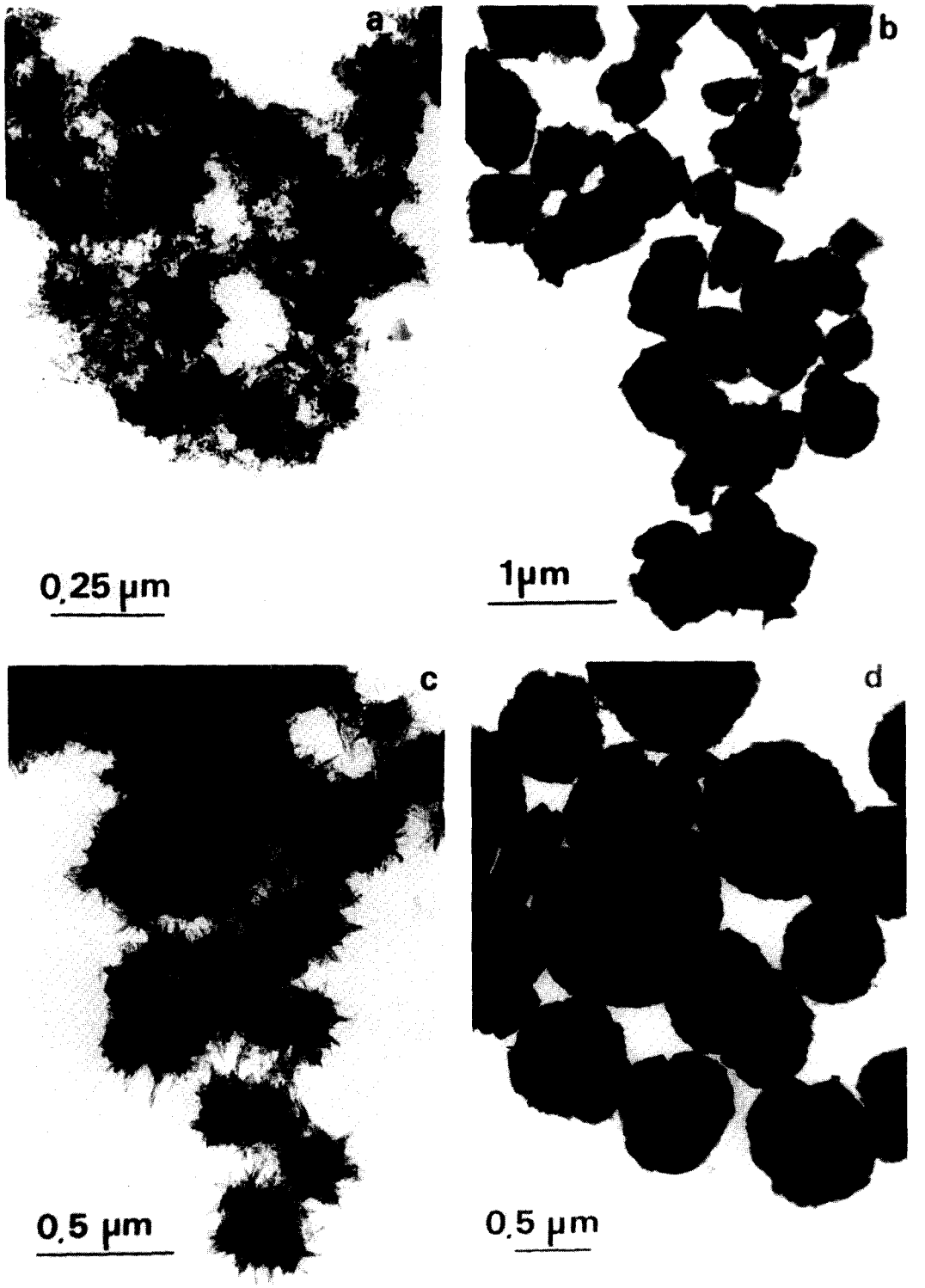

FIG. 1. Transmission electron micrographs of the tungsten hydrous oxide precursors and the corresponding metallic intermediates. (a) Metallic W obtained from the white precursor (×73,000); (b) metallic W obtained from the yellow precursor (×20,700); (c) white precursor ($WO_3 \cdot \frac{1}{3}H_2O$) (×43,200); (d) yellow precursor ($WO_3 \cdot H_2O$) (×24,300).

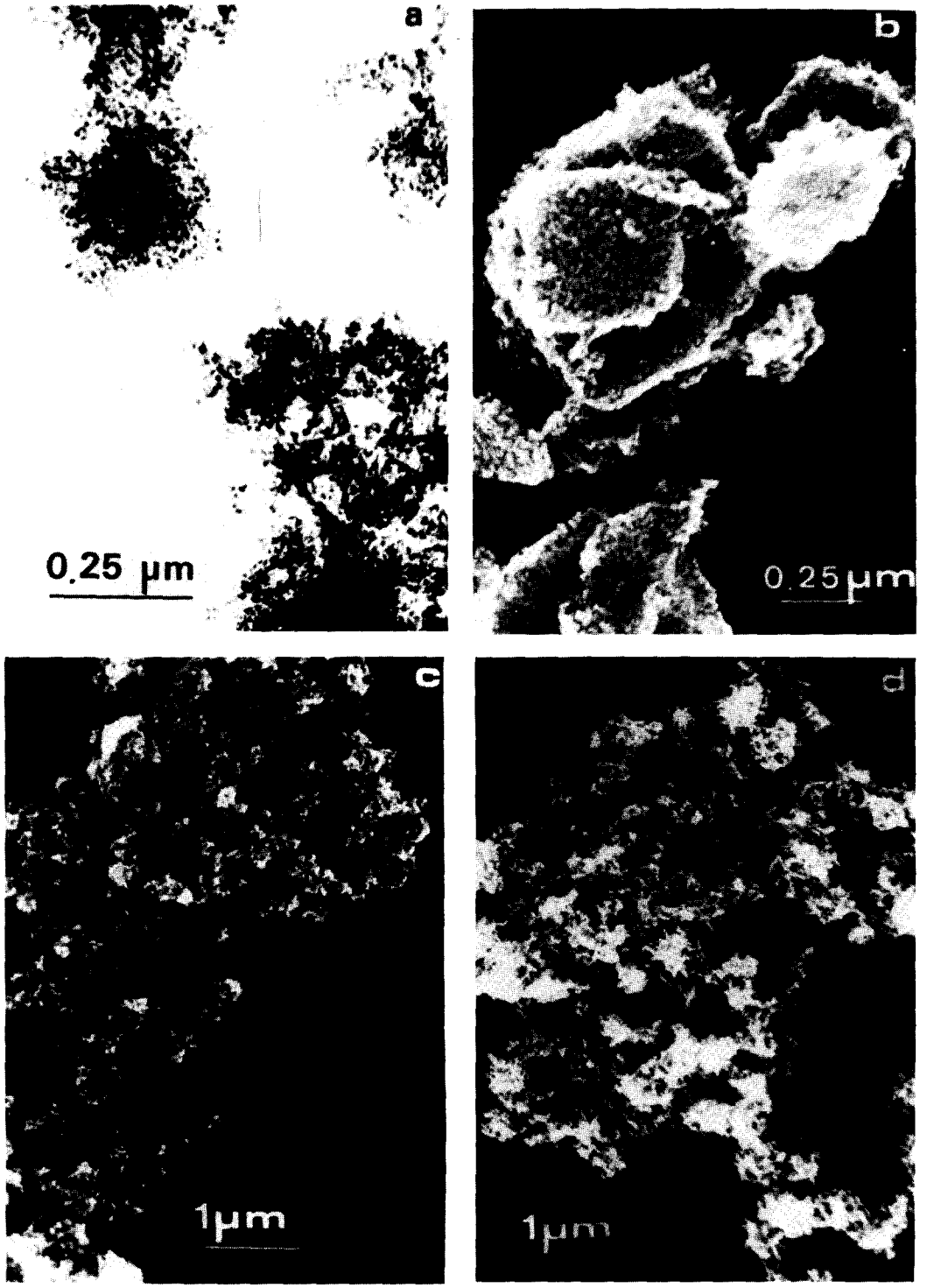

FIG. 2. Electron micrographs of tungsten carbide samples. (a) Wh-WC-CO (transmission; ×86,400); (b) Ye-WC-CO (scanning; ×54,000); (c) Wh-W_2C-wc (scanning, ×14,400); (d) Wh-WC-100 (scanning, ×21,600).

TABLE 2

Phase Composition and Surface Area of Carbide Samples Prepared in Pure CO

Expt. No.	Precursor	Temp. of reaction (°C)	Reaction time (h)	Composition (mol%)		Spec. surface area (m^2/g)
				W_2C	WC	
1	White	750	6	75	25	54
2	White	750	12	53	47	54
3	White	750	24	72	28	50
4	White	850	6	47	53	30
5	White[a]	850	12	0	100	47
6	Yellow	750	6	81	19	50
7	Yellow[b]	750	24	0	100	38
8	Yellow	850	12	44	56	—

[a] Sample referred to as Wh-WC-CO.
[b] Sample referred to as Ye-WC-CO.

same conditions, the transformation into WC of the yellow precursor is complete after 24 h (Experiments 6 and 7). At 850°C, on the contrary, the conversion to WC becomes complete within 12 h at 850°C only when the white precursor is used (compare Experiments 5 and 8).

Scanning electron micrographs of samples Wh-WC-CO (a) and Ye-WC-CO (b) are presented in Fig. 2; the former is made of loosely aggregated small particles, whereas the latter is composed of square platelets exhibiting marked surface roughness. No clear trend appears with respect to the influence of experimental conditions on the specific surface areas of the samples prepared in pure CO (see last column of Table 2).

The result of the XPS investigation of sample Wh-WC-CO is presented in Fig. 3 (curve C). The spectrum exhibits a single C 1*s* peak corresponding to a binding energy of 284.4 eV, very close to the value reported for graphite (285 eV) (*27, 28*).

Carburization in CO–CO_2 mixtures. Preliminary results are presented in Fig. 4A which shows how experimental conditions, (amount of solid in the reactor, flow rate of the gaseous reactants) can affect the kinetics of WC formation. For a given flow rate, a decrease of the reaction rate is observed when the amount of solid reactant is increased; moreover, the transformation goes back to W_2C for contact times longer than 30 h (compare curves 1 and 3). When both the flow rate and the amount of solid are increased the original kinetics of transformation are restored (compare curves 2 and 3).

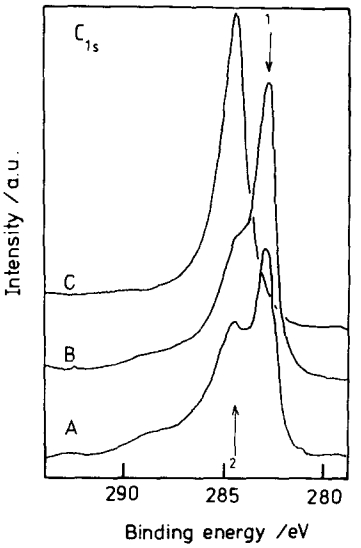

FIG. 3. XPS spectra of the C 1*s* level of WC samples. (A) Wh-WC-100, (B) Ye-WC-100, (C) Wh-WC-CO; (1) and (2) denote the binding energy for C 1*s* in WC and in graphite, respectively.

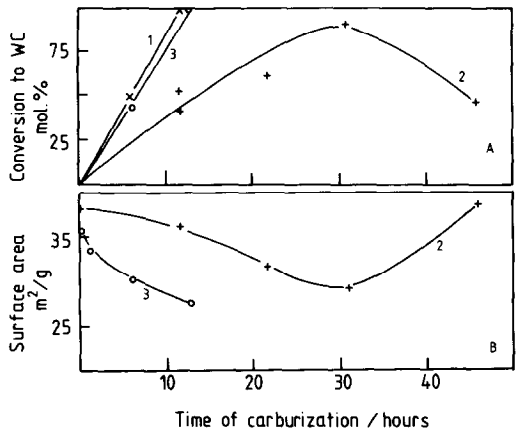

FIG. 4. Effects of Q, the weight of solid reactant and F, the gas flow rate on the change with time of the conversion to WC (A) and the specific surface area (B) of sample Wh-WC-x. Experimental conditions: T = 780°C; CO_2/CO = 0.1. (1) Q = 0.100 g, F = 22 liters/h; (2) Q = 0.400 g, F = 22 liters/h; (3) Q = 0.400 g, F = 31 liters/h.

The effects of temperature and gas phase composition on the conversion and the specific surface areas of the carburized samples are summarized in Table 3. In CO_2-rich mixtures (CO_2/CO = 0.5 or 1, Experiments 1–4), the carburization reaction stops at W_2C and reoxidation can even take place at higher temperature (Exp. 2). In CO_2-poor mixtures (CO_2/CO = 0.1, Experiments 5–12), the conversion to WC proceeds progressively and is complete after 13 h at 750°C.

The micrographs c and d of Fig. 2 show that the morphologies of samples Wh-WC_2-ic and Wh-WC-100 are very similar. Surface areas are presented in Table 3 (last column) and in Fig. 4B; the figure shows that the specific surface areas of the samples prepared using the highest flow rate tend to decrease with time (curve 3), and that the area goes through a minimum when a lower flow rate is used (curve 2).

The XPS results are presented in Fig. 3 (curves A and B). They show that samples Wh-WC-100 and Ye-WC-100 both exhibit a C 1s doublet; the main peak at E_b = 282.7 eV corresponds to the carbide phase (*18, 29*) while the shoulder at E_b = 284.5 eV can be assigned to free carbon as above.

DISCUSSION

Carburization Reactions

Thermodynamic equilibria. The limits of the domains of thermodynamic stability of WO_3, WO_2, W, W_2C, WC, and C expressed as the pressure ratio of CO_2 over CO versus the reciprocal of the absolute temperature,

TABLE 3

Phase Composition and Surface Area of Carbide Samples Prepared in CO–CO_2 Mixtures

Expt. No.	Sample	CO_2/CO ratio	Temp. (°C)	Time (h)	Composition (mol%)		Spec. surface area (m^2/g)
					W_2C	WC	
1	Wh-W_2C-1	1.0	750	24	100	0	—
2	Wh-WO_2	1.0	850	12	(WO_2)		—
3	Wh-W_2C-2	0.5	735	12	100	0	—
4	Wh-W_2C-wc[a]	0.5	750	24	100	0	33
5	Wh-W_2C-ic[a]	0.1	750	0.5	100	0	36
6	Wh-WC-14	0.1	780	1	86	14	32
7	Wh-WC-24	0.1	780	3	76	24	34
8	Wh-WC-55	0.1	780	6	45	55	30
9	Wh-WC-63	0.1	780	8	37	63	31
10	Wh-WC-70	0.1	780	10	30	70	29
11	Wh-WC-100	0.1	780	13	0	100	28
12	Ye-WC-100	0.1	780	13	0	100	20

[a] wc: "well crystallized"; ic: "ill crystallized."

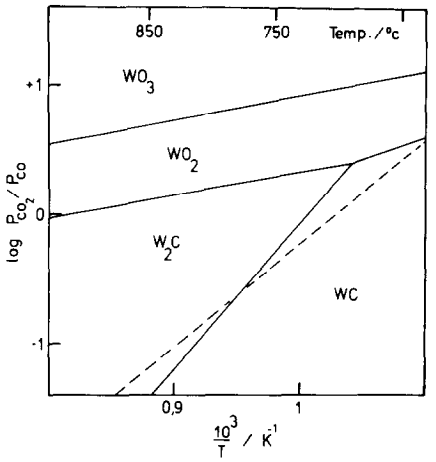

FIG. 5. Phase diagram of the system WO_3-WO_2-W_2C-WC-C [$\log(P_{CO_2}/P_{CO})$ versus the reciprocal of the absolute temperature] assuming p_{CO} = 1 atm. The dotted line represents the equilibrium of the Boudouard reaction: $2\,CO \rightleftharpoons CO_2 + C$.

are presented in Figs. 5 and 6. These phase diagrams have been calculated using the thermodynamic data given in Table 4, assuming p_{CO} = 1 atm. Fig. 5 corresponds to the situation in which the reacting gases have free access to the surface of the tungsten compounds. As a consequence of the Boudouard reaction ($2CO \rightarrow CO_2 + C$) free carbon deposition can occur to such an extent on the surface of the solid reactants that they become isolated from the gas phase. In that case the stability domains of the solid phases become independent of the composition of the gas phase below the Boudouard line; the corresponding phase diagram is presented in Fig. 6. As these diagrams show, the formation of WC free of excess carbon is thermodynamically possible provided suitable combinations of p_{CO_2}/p_{CO} ratios and temperatures are chosen.

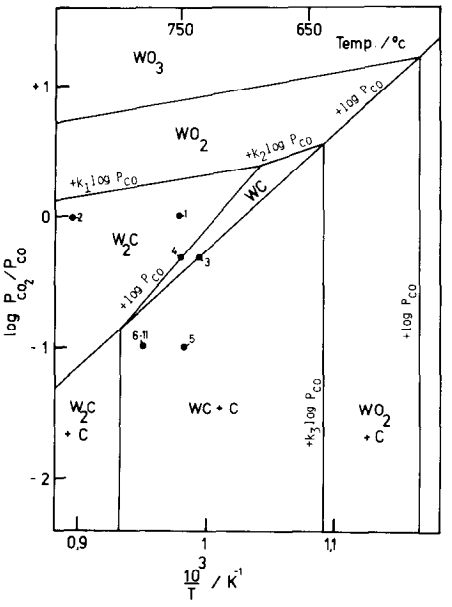

FIG. 6. Phase diagram of the system WO_3-WO_2-W-W_2C-WC-C assuming p_{CO} = 1 atm. The black dots correspond to the thermodynamic conditions of the experiments reported in Table 4 and are identified by the corresponding digit in the table (k_1 = 1/5; k_2 = 1/3; k_3 = 2).

TABLE 4

Thermodynamic Data Used for Establishing the Phase Diagrams of Figs. 5 and 6 (*30*)

Temp. (°C)	WO_3	WO_2	W	W_2C	WC	C
Values of the molar enthalpies of formation (kcal/mol) at P = 1 atm for different temperatures						
627	−188.396	−130.903	3.700	2.007	−3.143	2.319
727	−185.980	−129.070	4.354	4.420	−1.957	2.826
827	−183.222	−127.202	5.519	6.806	−0.751	3.345
Values of the molar entropies (cal/mol/K) at P = 1 atm for different temperatures						
627	41.017	30.065	14.520	43.020	19.233	5.327
727	44.062	31.996	15.219	45.499	20.482	5.861
827	46.691	33.776	15.853	47.774	21.631	6.355

Elementary reaction steps. The following reactions can be considered *a priori* to take place during the carburization of W:

$$2W + 2CO \rightleftharpoons W_2C + CO_2 \quad (1)$$

$$W_2C + 2CO \rightleftharpoons 2WC + CO_2 \quad (2)$$

$$2CO \rightleftharpoons C_{at} + CO_2 \quad (3)$$

$$W_2C + C_{at} \rightarrow 2WC \quad (4)$$

$$nC_{at} \rightarrow C_n \quad (5)$$

$$W_2C + 1/n\ C_n \rightarrow 2WC \quad (6)$$

Reactions (1) and (2) are direct solid–gas reactions. Reaction (3) is the Boudouard re-

action, in which C_{at} specifies atomic carbon (incipient carbon) species. Reaction (4) describes the solid state reaction between W_2C and atomic carbon. Incipient carbon can aggregate to polyatomic (pregraphitic) species through Reaction (5). Finally, W_2C can react with pregraphitic carbon through Reaction (6). This latter process requires very high temperatures (>1500°C) (*31*) to proceed at measurable rates so that its effect in the range of temperatures considered here (750–850°C) will be neglected.

Carburization in CO–CO_2 mixtures. For the sake of comparison of experimental results and thermodynamic predictions, each experiment presented in Table 3 has been represented in Fig. 6 by a solid circle carrying the corresponding number, the position of which is fixed by the thermodynamic conditions used (p_{CO_2}/p_{CO} ratio and temperature). Table 3 shows that, for reaction times beyond 12 h, the phase composition obtained corresponds to the thermodynamic equilibrium, except for Experiment 3 for which W_2C is obtained instead of WC as expected. Only experiments corresponding to points markedly below the Boudouard line (see Fig. 6) were found to produce WC. CO_2/CO ratios allowing the formation of free carbon through the Boudouard reaction (Reaction (3)) therefore appear to be necessary for obtaining WC. Accordingly, WC would not be produced through the direct gas–solid Reaction (2) but rather through Reactions (1), (3), and (4) in succession. This conclusion is substantiated by the XPS observations (see Fig. 3, curves A and B) showing the simultaneous occurrence of carbidic and free carbon species in the WC samples. Consequently, the formation of WC free of excess surface carbon would be possible provided that proper rates of Reactions (3), (4), and (5) can be established. Indeed, Reaction (5), which is presumably responsible for surface contamination of WC, will compete with Reaction (4) for consuming the incipient carbon produced by Reaction (3). The results presented in Fig. 4 can be tentatively explained in the light of the conclusions above. According to curve 2 of Fig. 4, the rate of carbide formation decreases when the amount of solid reactant is increased, other factors being kept constant. This effect can be ascribed to an increase of the CO_2/CO ratio at the solid–gas interface which will probably affect the kinetics of carbide formation, either by slackening Reaction (3) (the source of the incipient carbon consumed by Reaction (4) or by reversing the course of Reaction (2). The fact that Reaction (4) cannot go to completion indicates that Reaction (5) is less affected by the change of operating conditions so that the sample can be covered completely with an impervious layer of pregraphitic carbon before becoming completely converted to WC. The solid being thus isolated from the gas phase, only Reaction (6) could contribute to further formation of WC, which is unlikely in view of the low reaction temperature used (see above). Moreover, the decrease of WC conversion indicates that for isolated particles, Reaction (6) can take place backwards, pregraphitic carbon and W_2C being formed at the expense of WC. The change in the specific surface area (Fig. 4B) agrees well with the above interpretation since, as will be seen below, an increase of specific surface area upon carburization is correlated with free carbon formation. As a consequence of an increase of the flow rate (Fig. 4A, curve 3) CO_2 would be removed more efficiently from the solid–gas interface, thus restoring a higher rate of WC formation.

Carburization in pure CO. The preceding discussion indicates that the rate of carbon formation through the Boudouard reaction [Reaction (3)] depends on the CO_2/CO ratio at the solid–gas interface during the carburization process. In the case of carburization in pure CO this ratio will presumably depend on the rate at which the CO_2 molecules produced by Reactions (1) and (3) can be removed away from this interface. This rate will in turn depend on experimental factors such as the macroscopic flow rate of

gaseous reactants and the texture (particle size, porosity) of the solid reactants. Having this in mind we shall try to interpet the experimental data presented in Table 2, and address particularly the following questions:

(a) Why does the conversion to WC at 750°C go through a maximum in the case of the white precursor while the yellow precursor is completely converted to WC in the same conditions?
(b) Why is the white precursor converted completely to WC within 12 h at 850°C while the yellow one is not?

Figure 1 shows that the metallic tungsten intermediate is in the form of either needle-shaped, nonporous particles (white precursor, micrograph a) or of porous aggregates of platelets (yellow precursor, micrograph b). That the sample obtained from the yellow precursor is porous is further substantiated by the fact that, contrary to the white precursor, its specific surface area increases markedly upon reduction (see Table 1), probably due to the more massive shape of the particles and to the higher amount of hydration water evolved from the former precursor as compared with the latter. In the case of the nonporous solid it is likely that the CO_2/CO ratio existing at the solid–gas interface will be so low that free carbon formation through Reaction (3) will be much faster than its consumption through Reaction (4), which involves a slow diffusion process. The free carbon in excess is then likely to polymerize through Reaction (5) and to form an impervious layer of pregraphitic carbon. The solid particles will thus stop to transform as soon as they become isolated from the gas phase by such a carbon layer. This effect is magnified by the fact, mentioned already, that WC cannot be formed in the present conditions through a solid-state reaction such as Reaction (6). The backwards transformation to W_2C for contact times above 12 h (Table 2, Experiment 3) is difficult to explain at present on pure thermodynamic grounds. However, we may speculate that such a difference exists between the surface free energies of the WC/C and W_2C/C interfaces that WC would be unstable relative to W_2C in highly dispersed systems isolated from a $CO–CO_2$ atmosphere. As a consequence WC would convert to W_2C and free carbon through Reaction (6) proceeding backwards.

In the case of the porous solid prepared using the yellow precursor (see Table 2, Experiments 6 and 7), the elimination of CO_2 produced by Reactions (1) and (3) is likely to be limited by gaseous diffusion through the inner pores of the particles. A steady-state partial pressure of CO_2 would thus result which would presumably slow down the formation of free carbon through Reaction (3), and so limit the formation of an impervious carbon layer through Reaction (5) to such an extent that the conversion of the sample to WC is not hindered.

The fact that the white sample is completely converted to WC within 12 h at 850°C (see Table 2, Experiments 4 and 5) indicates a different sensitivity to temperature of Reactions (4) and (5). Indeed, the activation energies reported in the literature are 40 kcal/mol for Reaction (4) (*18, 32*) (assuming a mechanism involving dissolution and diffusion of C in the W_2C lattice) and 20 kcal/mol for Reaction (3) (*33*). A higher proportion of carbon produced by Reaction (3) is thus likely to react to form WC instead of contributing to the formation of a free carbon coating. Table 3 (Experiments 6–8) shows that the rate of transformation of the yellow precursor is very little sensitive to temperature changes, since the conversion observed after 12 h at 850°C is only slightly higher than the interpolated value corresponding to the same contact time at 750°C (56 vs 50%). This result confirms the previous hypothesis that the reaction is controlled by a gas-phase diffusion process within the porosity of this sample. Indeed, using 4 kcal/mol as a representative value for the activation energy of gas-phase diffusions, it is easy to calculate that a tem-

perature increase from 750 to 850°C would accelerate the reaction by a factor of 1.2 only. Another possible cause of reaction slackening in the present case would be the obstruction of pore openings due to the thermal acceleration of carbon deposition at the outer surface of the particles.

At the end of the present section it is worth noting that pregraphitic carbon is always observed during carburization in pure CO. The XPS analysis of sample Wh-WC-CO (Experiment 5 of Table 2) shows that the binding energy of the only C 1*s* peak observable corresponds to graphitic carbon; this result points to an extensive coating of the solid by a continuous layer of carbon. On the other hand, free carbon deposition seems to be responsible for the increase of specific surface area observed in Fig. 4B beyond the reaction time corresponding to the maximum conversion to WC. This is confirmed by the higher specific surface areas generally presented by the samples prepared in pure CO as compared to those prepared in $CO–CO_2$ mixtures.

Dispersion of Tungsten Carbides and Intermediary Compounds

The results presented here show that it is possible to prepare tungsten carbides exhibiting specific surface areas higher than those generally reported in the literature (see Table 5). Moreover, literature values correspond to samples prepared in pure CO or $CO–H_2$ mixtures. Therefore, some of the areas could have been overestimated because of the possible contribution of large amounts of free excess carbon.

The highest specific surface areas observed in the present work might appear low when comparison is made with the values usually obtained for catalyst supports such as SiO_2 or Al_2O_3 (150 to 300 m^2/g). However, the direct comparison of specific surface areas of WC and SiO_2 is distorted due to their very different densities. The actual dispersion state obtained for the samples presented here is best illustrated by comparing their specific surface areas to those of reference samples having the same particle sizes. This comparison is made in Table 6, where the reader can see that the carbides, precursors and other intermediate solids prepared in this work are comparable, from the point of view of dispersion, to highly dispersed silicas.

TABLE 5

Comparison of the Degree of Dispersion of WC Samples with Values Reported in the Literature

Precursor or sample	Specific surface area of the final carbide (m_2/g)	Reference
White modification	5 to 16	*21*
Yellow modification	3 to 12	*21*
Yellow modification	15	*18*
WCl_6	3.5	*27*
Tungstic acid	32	*36*
W metal	30	*35*
W metal	2 to 4	*34*
Wh-WC-CO	47	This work
Wh-WC-100	28	This work
Ye-WC-100	20	This work

CONCLUSIONS

This work shows that highly dispersed tungsten carbides, free of excess carbon can be prepared by reduction in hydrogen of appropriate precursors and subsequent carburization in $CO–CO_2$ mixtures. Whatever the kind of precursor used, carburization in pure CO always results in samples contaminated with large amounts of pregraphitic carbon which could in some instances impede their complete conversion to WC. The dispersion state of the final carbides is mainly determined by the nature of the starting precursor. The carburization conditions have to be adatped to the texture of the precursor actually used in order to obtain the complete conversion of the sample without excessive contamination by free carbon. As a result of this controlled preparation, WC samples have been obtained in a state of dispersion such that it can be compared to that of silica supports having high specific surface areas.

TABLE 6

Comparison of the Degree of Dispersion of WC Samples and Intermediate Compounds Prepared in This Work with Silicas Having the Same Particle Shape and Size

Sample	Density (g/cm^3)	Spec. surface area (m^2/g)	Particle size (nm)	Equivalent SiO_2 spec. surface area[a] (m^2/g)
Yellow prec.	7.16	16	52.4	52
White prec.	7.16	82	10.2	267
Ye-W metal	19.3	64	4.9	557
Wh-W metal	19.3	71	4.4	620
Wh-WC-100	15.6	28	13.7	199

[a] Specific surface areas (m^2/g) calculated using the formula

$$S = 6000/(D \times \rho),$$

where D (nm) is the particle size and ρ the density of silica (2.2 g/cm^3).

ACKNOWLEDGMENTS

We thank M. Genet for assistance in electron microscopy. J. Lemaître thanks the Belgian Fund for Scientific Research (FNRS) for financial support. B. Vidick thanks IRSIA for a doctorate grant. Thanks are also due to L. Boogaerts and C. Pierard for technical assistance.

REFERENCES

1. Muller, J. M., and Gault, F. G., *Bull. Soc. Chim. Fr.* **2,** 416 (1970).
2. Sinfelt, J. H., and Yates, D. J. C., *Nature Phys. Sci.* **27,** 229 (1971).
3. Levy, R. B., and Boudart, M., *Science (Washington)* **181,** 547 (1973).
4. Vertes, G., Horanyi, G., and Szakacs, S., *J. Chem. Soc. Perkin Trans. 2,* 1400 (1973).
5. Ilchenko, N. I., *Kinet. Katal.* **18,** 153 (1977).
6. Ilchenko, N. I., *Kinet. Katal.* **14,** 976 (1973).
7. Kojima, I., Miyazaki, E., Inoue, Y., and Yasumori, I., *J. Catal.* **59,** 472 (1979).
8. Vertes, G., Horanyi, G., and Diss, G. Y., *Acta Chim. Acad. Sci. Hung.* **83,** 135 (1974).
9. Astier, M., Bertrand, P., and Teichner, S. J., *Bull. Soc. Chim. Fr.* **5–6,** 205 (1980).
10. Voorhies, J. D., *J. Electrochem. Soc.* **119,** 219 (1972).
11. Armstrong, R. D., Douglas, A. F., and Keene, D. E., *J. Electrochem. Soc.* **118,** 568 (1971).
12. Böhm, H., *Electrochem. Acta* **15,** 1273 (1970).
13. Fleischmann, R., and Böhm, H., *Ber. Bunsenges. Phys. Chem.* **84,** 1023 (1980).
14. Mills, G. A., and Steffgen, F. W., *Catal. Rev.* **8,** 159 (1973).
15. Böhm, H., and Pöhl, F., *in* C.R. 3èmes J. Int. Piles à Combustibles, Brussels, June 1969 (SERAI and COMASCI, Eds.), p. 183. Presses Académiques Européenes, Brussels, 1969.
16. Palanker, V. S. H., Gayev, R. A., and Sokolsky, D. V., *Electrochem. Acta* **22,** 133 (1977).
17. Böhm, H., Ger. Offen. 2106599, 17 Aug. 1972, Appl. P. 2106599. 6, 12 Feb. 1971.
18. Ross, P. N., and Stonehart, P., *J. Catal.* **48,** 42 (1977).
19. Leclercq, L., Imura, K., Yoshida, S., Barbee, T., and Boudart, M., *in* "Preparation of Catalysis II" (B. Delmon, P. Grange, P. Jacobs, and G. Poncelet, Eds.), p. 627. Elsevier, Amsterdam, 1979.
20. Ross, P. N., and Stonehart, P., *J. Catal.* **39,** 298 (1975).
21. Nikolov, I., Nikolova, V., and Vitanov, T., *J. Power Sources* **4,** 65 (1979).
22. Nikolov, I., Suata, M., Grigorov, L., Vitanov, T., and Zabransky, Z., *J. Power Sources* **3,** 237 (1978).
23. Nikolov, I., Vitanov, T., and Nikolova, V., *J. Power Sources* **5,** 197 (1980).
24. Nikolov, I., Nikolova, V., and Vitanov, T., *J. Power Sources* **7,** 83 (1981/1982).
25. Vidick, B., PhD thesis. Faculté des Sciences Agronomiques, Université Catholique de Louvain, Louvain la Neuve, 1984.
26. Kervyn, G., Lemaître, J., and Delmon, B., *in* "Proceedings, 4th Int. Conf. Surface and Colloid Sci., Jerusalem 1981," Abstract 114, p. 227.
27. Ramquist, L., Hamrin, K., Johansson, G., Fahbman, A., and Nordling, C., *J. Phys. Chem. Solids* **30,** 1835 (1969).
28. Johansson, G., Edman, J., Berudtsson, A., Klassov, M., and Nilsson, R., *J. Electron Spectrosc. Relat. Phenom.* **2,** 295 (1973).
29. Miles, R., *J. Chem. Technol. Biotechnol.* **30,** 35 (1980).
30. Barin, I., and Knacke, O., "Thermochemical Properties of Inorganic Substances," Springer-Verlag, New York, 1973.
31. Schwartzkopf, P., and Kieffer, R., "Refractory Hard Metals." MacMillan, New York, 1953.
32. Kovenski, I. I., "Diffusion in Body-Central Cubic Metals," p. 286. Amer. Soc. Metals, Metals Park, Ohio, 1965.
33. Karcher, W., and Glande, P., *in* Biennal Conf. Carbon, Ext. Abstr. Program 11th, 1973 (CONF-730601) NTIS: p. 43, Springfield, Va.
34. Zvata, M., and Zabranski, Z., *Collect. Czech, Chem. Commun.* **39,** 1015 (1974).
35. Mazklevski, E. A., Palanker, V. S. H., and Domanovskaya, E. I., *Kinet. Katal.* **18,** 1967 (1977).
36. Palanker, V. S. H., *in* Ext. Abstr. Meet. Int. Soc. Electrochem. 28th 1977; Sofia (R. V. Moshtev, Ed.), Vol. 2, p. 276.